

# Multilevel musculo-fascial defect magnetic resonance study of female pelvic floor: retrospective case control study in women with pelvic floor dysfunction after the first vaginal delivery

Michal Krčmar<sup>1,2</sup> | Lukas Horcicka<sup>2</sup> | Martin Nemec<sup>2</sup> | Petra Hanulikova<sup>1</sup> | Jaroslav Feyereis<sup>1,2</sup> | Ladislav Krofta<sup>1,2</sup> 

<sup>1</sup>3<sup>rd</sup> Medical Faculty, Charles University, Prague, Czech Republic

<sup>2</sup>Institute for the Care of Mother and Child, Prague, Czech Republic

## Correspondence

Ladislav Krofta, Institute for the Care of Mother and Child, Podolske nabrezi 157, Prague 4, 14700, Czech Republic.  
Email: [ladislav.krofta@post.cz](mailto:ladislav.krofta@post.cz)

## Funding information

3<sup>rd</sup> medical faculty, Charles University, Prague, Grant/Award Number: PROGRES

## Abstract

**Introduction:** Magnetic resonance imaging (MRI) provides a detailed display of the pelvic floor structures responsible for normal pelvic floor anatomy. The aim of the study is to assess the appearance of musculo-fascial defects in women with pelvic floor dysfunction following first vaginal delivery.

**Material and methods:** Analysis of axial T3 (Tesla 3) MRI scans from a case control study of symptomatic ( $n = 149$ ) and asymptomatic ( $n = 60$ ) women after first vaginal delivery. Presence and severity of pelvic organ support and attachment system defects in three axial pelvic planes were assessed.

**Results:** In the symptomatic group, major muscular defects were found in 67.1% (for pubovisceral muscle complex) and 87.9% (for iliococcygeal muscle). Only 6.7% of major pubovisceral and 35.0% of major iliococcygeal defects were identified in the controls ( $p = 0.000$ ). Prolapse patients had an odds ratio (OR) of 22.1 (95% CI 8.94–54.67) to have major pubovisceral muscle complex defect and OR of 4.9 (95% CI 1.51–15.71) to have major iliococcygeal muscle defect. Fascial defects were found in 60.4% and 83.2% the symptomatic group, respectively. Those with prolapse had an OR of 29.1 (95% CI 9.77–86.31) to have facial defect at the level of pubovisceral muscle complex and an OR of 16.9 (95% CI 7.62–37.69) to have fascial defect at the level of iliococcygeal muscle. Uterosacral ligaments detachment was associated with prolapse with an OR of 10.1 (95% CI 4.01–25.29). For the model based on combination on all MRI markers, the area under the receiver operating characteristic curve is 0.921.

**Conclusions:** This study provides comprehensive data about first vaginal delivery-induced changes in the levator ani muscle and endopelvic fascial attachment system.

**Abbreviations:** AD, architectural distortion; APL, arcuate pubic ligament; AUC, area under the curve; CT, connective tissue; FA, full avulsion; ICM, iliococcygeal muscle; LAM, levator ani muscle; MRI, magnetic resonance imaging.; OIM, obturator internus muscle; OR, odds ratio; P1, plane 1; P2, plane 2; P3, plane 3; PFD, pelvic floor dysfunction; PMC, pubovisceral muscle complex; POP, pelvic organ prolapse; POP-Q, pelvic organ prolapse quantification; PRM, puborectal muscle; ROC, receiver operating characteristic curve; T3, Tesla 3; USL, uterosacral ligaments; VD, vaginal delivery.

This is an open access article under the terms of the [Creative Commons Attribution-NonCommercial-NoDerivs](https://creativecommons.org/licenses/by-nc-nd/4.0/) License, which permits use and distribution in any medium, provided the original work is properly cited, the use is non-commercial and no modifications or adaptations are made.

© 2022 The Authors. *Acta Obstetrica et Gynecologica Scandinavica* published by John Wiley & Sons Ltd on behalf of Nordic Federation of Societies of Obstetrics and Gynecology (NFOG).

These changes are seen also in asymptomatic controls, but they are significantly less expressed.

#### KEYWORDS

architectural distortion, delivery, levator ani muscle, magnetic resonance imaging, prolapse

## 1 | INTRODUCTION

It is accepted that vaginal delivery (VD) may result in trauma to the levator ani muscle (LAM).<sup>1</sup> In high-risk groups, 30%–65% of women show signs of LAM injuries.<sup>2</sup> The LAM has three subdivisions: pubovisceral, puborectal and iliococcygeal. Our understanding of the mechanical effects that result from LAM trauma, and why that is linked to the development of pelvic floor dysfunction (PFD), is at present poor. Recent advances in magnetic resonance imaging (MRI) have proved that knowledge of the pelvic floor muscles and connective tissue (CT) can help understanding the etiology of PFD.<sup>3,4</sup> MRI measurements and comparisons are possible because of the use of a standardized investigation technique. A scoring system was created to describe LAM injuries seen with MRI.<sup>5</sup> Women with pelvic organ prolapse (POP) have an odds ratio (OR) of 7.3 of having LAM defects seen on MRI compared with women without prolapse.<sup>4</sup> CT elements are also an important part of the support system and their disorders are considered a contributing mechanism in POP.<sup>6</sup> At present, the morphologic appearance of injured or damaged CT in MRI scans is not as well understood in the assessment of pelvic floor damage.<sup>7</sup>

The aim of this study was to explore the status of musculo-fascial pelvic floor structures after first VD, so as to understand the damage caused by this delivery and its relation to PFD.

## 2 | MATERIAL AND METHODS

### 2.1 | Study design, sample size

A retrospective observational case controlled single-center study was conducted between November 2014 and September 2018 in the Institute for the Care of Mother and Child in Prague. This is a tertiary perinatal center which conducts over 5000 deliveries per year and admits pregnant women from all regions of the Czech Republic. In the capital city alone, the institute manages 25% of all deliveries. During the study period, 268 women were referred to the institutional urogynecologic outpatient clinic with PFD after first VD. Inclusion criteria were met by 149 (55.6%) women. The reason for exclusion was multiparity (37.7%) and a history of previous cesarean section (6.7%). The control group consisted of 60 women. Informed consent was obtained from all participants. Inclusion criteria for symptomatic women were: (a) first vaginal singleton delivery at or beyond 37 weeks, including instrumental (any type of forceps or vacuum extraction), (b) PFD symptoms developing following

#### Key message

Pelvic floor damage after first vaginal delivery, as verified by magnetic resonance imaging, is significantly more frequent in patients with pelvic floor dysfunction.

delivery, (c) minimal interval of 6 months from VD. The types of PFD were as follows: urinary incontinence symptoms, vaginal prolapse symptoms, anorectal dysfunction symptoms and dyspareunia/vaginal laxity. The study group was recruited on the basis of PFD symptoms. Validated Czech version questionnaires (ICIQ-SF, PISQ-12) were used to quantify PFD symptoms. The control group consisted of women following uncomplicated VD. Uncomplicated VD was defined as spontaneous, vertex and between 37 and 42 weeks of pregnancy. Control subjects were required to have their most dependent pelvic organ prolapse-quantification (POP-Q) point 2.0 cm or more above the hymenal ring remnant during a Valsalva maneuver and to lack PFD symptoms. Exclusion criteria for both groups were: (a) multiparity, (b) previous vaginal or perineal surgery, (c) being non-Caucasian.

### 2.2 | Procedures, data analysis and outcome measures

The anatomical assessment was performed with the POP-Q classification system.<sup>8</sup> The MRI imaging protocol was a high-resolution T3 MRI scan (Phillips Achieva TX series), taken in the supine position. The imaging parameters were as follows: repetition time 5331 msec, 375 phase encodes, 24-cm field of view, and 2-mm slice thickness, no gap between slices in axial, coronal or sagittal projections. MRI sequences at rest were acquired in sagittal, coronal and axial planes. Axial images display at best the relationship between the genital tract and pelvic walls at each level including the nature of the attachments.<sup>13</sup> The women had not received bowel or bladder preparation and had urinate 30 min before the examination.

On initial review, scans that appeared to have abnormalities were presumptively identified based on the comparison with normal anatomy of pelvic floor previously described by the group of DeLancey.<sup>9,10</sup> All scans were evaluated independently by two researchers (M.K., L.K.) blinded to subjects' POP-Q status and PFD symptoms. Final classification of LAM or CT was only established when abnormal LAM and/or CT morphology was found as agreed

upon by the two investigators. When the two examiners disagreed in the presence of an abnormality, re-examination of the scans was performed. New examiner (M.N.) viewed the questionable scans blinded to previous evaluations.

We observed the severity of LAM and CT defects in most distally placed evaluation plane 1 (P1) and proximally located plane 2 (P2). The most cephalad plane 3 (P3) was used only for the assessment of CT defects. For P1 reference structure, the arcuate pubic ligament (APL) was chosen. Axial scans in P1 were used for the evaluation of pubovisceral muscle complex (PMC) and the presence of “architectural distortion” (AD). Isolated evaluation of the puborectal muscle (PRM) was not performed. Under normal conditions in the axial scans the PMC can be seen arising from the pubic bone lateral to the urethra, vagina and rectum and medial to the obturator internus muscle (OIM). AD represents abnormal lateral dislocation of the vaginal wall in the peri-urethral region. It is associated with posterior extension of the space of Retzius and demonstrates CT disruption.<sup>5</sup> PMC was observed in three slices cranial and caudal to the APL. PMC defects were scored using a previously described method.<sup>11</sup> The right and left LAM portions were scored separately (Figure 1). The resulting grade is the sum of the scores of the right and left sides (grade 0: no defect, grade 1–3: minor defect, grade 4–6: major defect). Unilateral grade 3 defect was considered to be a major unilateral defect. Full avulsion (FA) injury was diagnosed within the LAM defect if there was a missing LAM attachment to the pelvic side wall as well as the loss of the hammock-like shaped vagina on the same side. Due to the combination of musculo-fascial trauma, the vagina protrudes laterally in the direction of OIM. The result is a deconfiguration of the typical vaginal shape. AD was classified as present or absent. Based on these results in P1, all subjects were then categorized into one of five groups: (i) normal LAM and no AD, (ii) LAM defect grade 1–3 (bilateral minor defect) and no AD, (iii) LAM defect grade 1–3 (bilateral minor defect) and AD = FA injury, (iv) LAM defect grade 4–6 bilateral (or 3 unilateral) and no AD (bilateral or unilateral major defect), (v) LAM defect grade 4–6 bilateral (or 3 unilateral) and AD = bilateral or unilateral FA injury.

At P2, the ileococcygeal muscle (ICM) was examined. The bladder base was chosen as the reference structure. The same scoring system for musculo-fascial trauma assessment in P1 was used in P2 (Figure 1).

In P3 we assessed the CT visibility according to the origins of the uterosacral ligaments (USL) and insertion points.<sup>12,13</sup> The ischial spine was chosen as the reference structure. All USL relevant structures were assessed from ischial spine in a cranial direction. Both origin/insertion points should be simultaneously visible in at least one axial section (Figure 2). Based on these results in P3, all subjects were categorized into one of three groups: (i) normal USL origin/insertion points, (ii) abnormal USL origin/insertion points, (iii) the USL condensation is not detectable. Abnormal USL origin/insertion points were defined as follows: in the investigated plane, the points were visible only on one side (left or right), or the right and left origin/insertion points could not be displayed simultaneously in one plane.

Primary outcome was the analysis of musculo-fascial defects at P1, P2 and fascial defects at P3 in the symptomatic and control groups. Secondary outcomes included the analysis of defect type localization relating to POP-Q parameters.

## 2.3 | Statistical analyses

All statistical analyses were performed using SPSS software version 19.0 (SPSS Inc.) IBM SPSS Sample Power version 3 (IBM) and G\*POWER version 3.1.9.2 (Kiel/University). The symptomatic and asymptomatic groups were compared; OR and multivariable logistic regression analysis were performed as well as the chi-square test of homogeneity. For continuous, normally distributed variables, Student's *t*-test was used. The non-parametric tests (Wilcoxon–Mann–Whitney test) were used for continuous, non-normally distributed variables. Fisher's exact test was used to test the independence in the contingency table with dichotomous variables. Fisher's exact test is generalized to RxC Tables. A *p*-value <0.05 was considered to be significant. We used receiver-operating characteristic (ROC) analysis to determine the predictive value of combining factors that were predictors of PFD. A post hoc power calculation was performed. The power of a test was computed for observed effect size. Using the intraclass correlation coefficient, interobserver (L.K. and M.K.) agreement was obtained for all parameters at P1, P2 and P3 in a test/retest series in blinded way on 76 women.

## 2.4 | Ethical approval

This study was approved by the institutional scientific and ethics committee (EK ÚPMD 3/2013) on October 3, 2013.

## 3 | RESULTS

During the study period inclusion criteria were met by 149 women. The control group consisted of 60 women. Demographic and clinical information is listed in Table 1. The mean time interval from VD to the examination for PFD symptoms in our institution was 13.5 months (min. 7, max. 36). Twenty-six (17.5%) subjects in the symptomatic group had an instrumental delivery (Simpson 5.4%, Breus 3.4%, Kjelland 5.4%); no such type of delivery was found in the control group. The most common PFD symptom was POP 95/149 (63.8%). In 103/120 (85.8%) women with POP, the anterior-predominant prolapse was more likely to be involved in the defect.

The intraclass correlation coefficient comprised 45 symptomatic and 31 asymptomatic MRI examinations. The values were ranked between 0.59 and 0.96, with the best agreement for the LAM and CT defects at P1 and P2. The lowest agreement concerned the evaluation of the left USL origin/insertion points (Table 2).

The incidence and distribution of each type of LAM and CT defect are shown in Table 3. Bilateral major LAM defect at P1 occurred

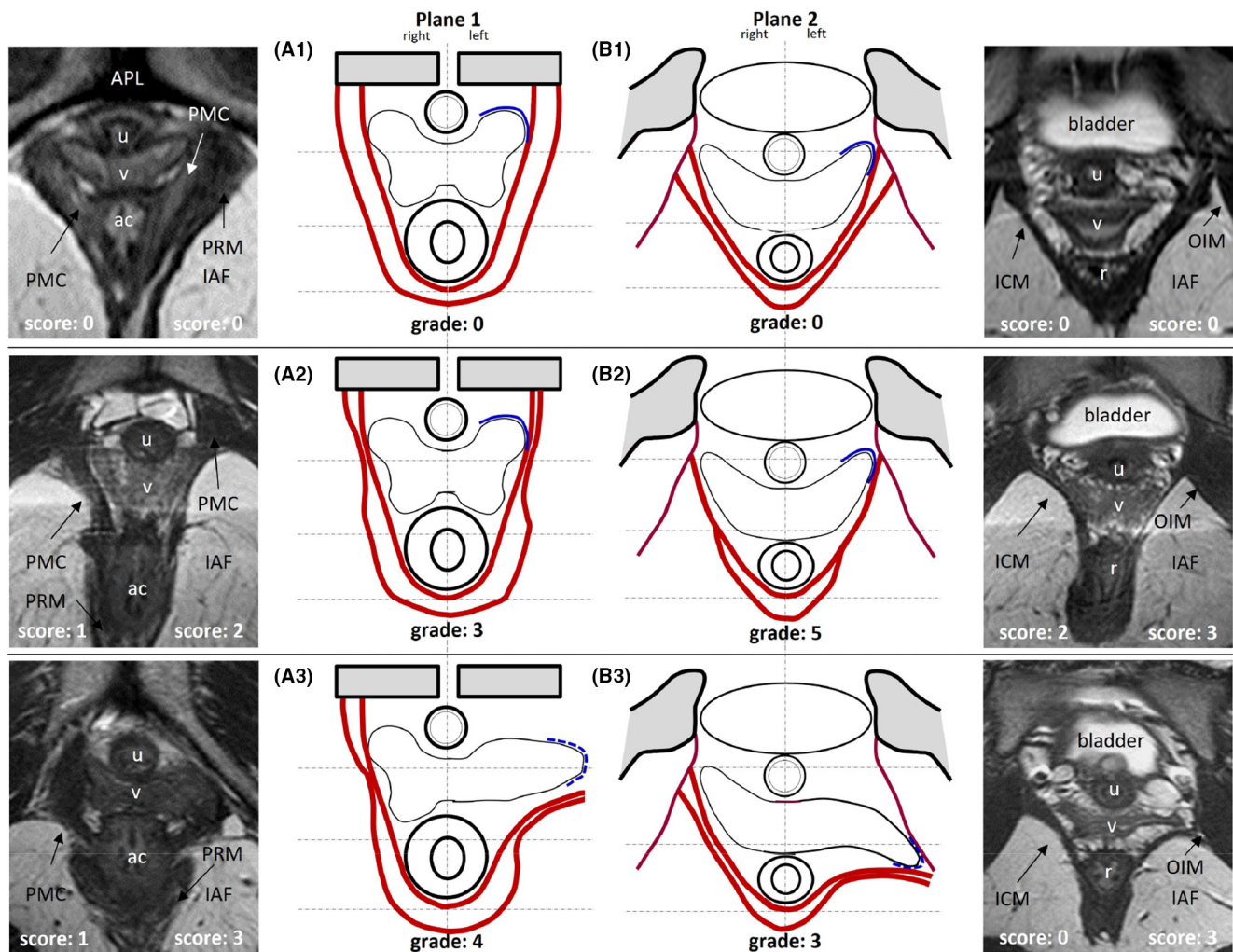


**FIGURE 1** Axial T3 MRI images showing PMC/PRM (A) and ICM (B) portions of the LAM. The simplification scheme shows the LAM as a whole, without highlighting subdivisions. The sections in (A) are placed at the level of APL. The sections in (B) are placed at the level of proximal urethra and bladder base. The grade of LAM defects are noted at the bottom of the scheme pictures. The score for each side is indicated on the MRI image. The right and left portions are scored separately. A score of "0" is assigned if no damage is visible. A score of "1" or "2" is assigned respectively if more or less than one half of the muscle is missing. Where the complete muscle bulk is lost, the score is "3". The resulting grade is the sum of the scores of the right and left side. The minimum score is 0, the maximum is 6, and categorization of scores as follows: grade 0—no defect, grade 1–3—minor defect, grade 4–6—major defect. Unilateral grade 3 defect is a major unilateral defect. (A1, B1) A 27-year-old nulliparous woman. (A1) Normal bilateral attachment of the PVM to the pubic bone, normal muscle bulk and vaginal wall architecture (grade 0). (B1) Normal appearance of the ICM; note the attachment of the muscle to the OIM (grade 0—LAM defect is not present). (A2, B2) A 30-year-old primiparous woman. (A2) Bilateral loss of muscle bulk but preservation of vaginal wall architecture; the muscle bulk loss is more pronounced on the left side (grade 3 defect—minor LAM defect). The bulk of the LAM is lost and the connection to the bone remains intact. (B2) Bilateral thinning of the ICM but normal muscle attachment; the muscle thinning is more pronounced on the left site (grade 5 defect—major LAM defect). (A3, B3) A 29-year-old primiparous woman. (A3) Normal right attachment of the PMC to the pubic bone with minor loss of muscle bulk (score 1); the normal attachment of the muscle to the pubic bone on the left side is missing, the ventral part of the PMC is shifted dorso-laterally, and due to the combination of musculo-fascial trauma, the vagina protrudes laterally and reaches the obturator internus muscle (grade 4 defect—major LAM defect). (B3) The defect reaches the ICM. The left vaginal wall lies close to the OIM (grade 3 defect—major unilateral LAM defect). In total: left-sided FA injury at P1 and P2. ac, anal canal; APL, arcuate pubic ligament; FA, full avulsion; IAF, ischioanal fossa; ICM, iliooccygeal muscle; MRI, magnetic resonance imaging; OIM, obturator internus muscle; PMC, pubovisceral muscle complex; PRM, puborectal muscle; r, rectum; T3, Tesla 3; u, urethra; v, vagina

simultaneously with bilateral major LAM defects at P2 in 68/70 (97.1%) cases.

Multivariable logistic regression was used to identify which characteristics independently predict POP development after first VD

(Table 4). The final model includes a combination of LAM morphology at P1 and P2, AD at P1 and P2, and USL morphology at P3. The ROC area under the curve (AUC) for the model based on a combination of all parameters was 0.921 (Figure 3).



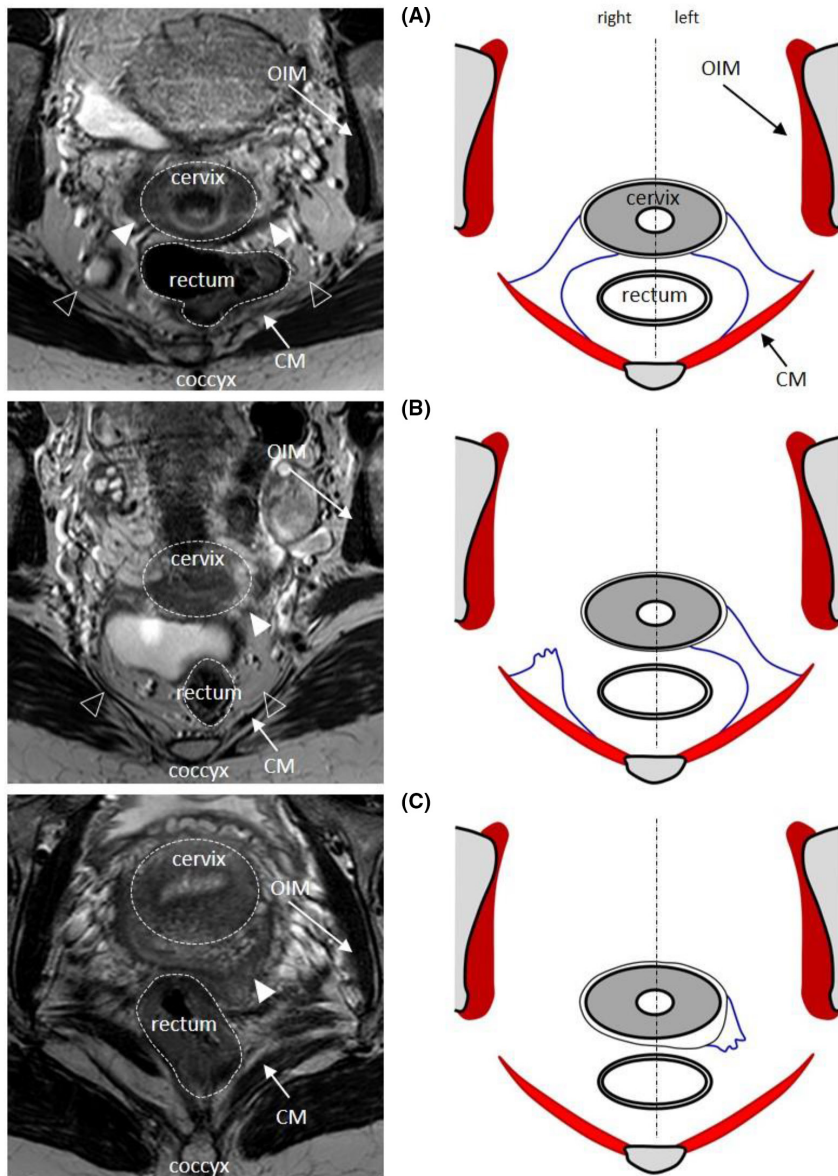


**FIGURE 2** Axial 3T MRI images at the level of the cervix and appropriate scheme showing USL origins and insertions. Origin was defined as the point where the CT condensed to a band-like structure at the dorsal margin of the uterine cervix and/or at the upper third of the posterior vaginal wall. Insertion was defined as the point at the pelvic sidewall where the CT ended. Both origin/insertion points should be simultaneously visible at least in one axial section. (A) A 27-year-old nulliparous woman. The full arrowheads demonstrate the origin of the CT from the cervix, their insertions on the pelvic sidewall are also seen (open arrowheads). (B) A 32-year-old primiparous woman with central defect stage II. Only the left ligament origin/insertion points (full/open arrowheads) are visible; on the right side only the insertion point is visible. (C) A 30-year-old primiparous woman with central defect stage III with abnormal uterosacral ligament anatomy; on the left side, only the insertion point (full arrowheads) is visible. On the right, origins-insertion points are not detectable. 3T, Tesla 3; CM, coccygeal muscle; CT, connective tissue; MRI, magnetic resonance imaging; OIM, obturator internus muscle; USL, uterosacral ligaments

## 4 | DISCUSSION

This study provides insight into the effect of first VD on the pelvic organ support and attachment system.<sup>6</sup>

In all, 80.5% of symptomatic women showed signs of POP, the most common being POP symptoms in 95/149 (63.8%); therefore some women with a clinical sign of POP do not show symptoms of POP. These women with POP-Q stages I and II who had other types of PFD symptoms. This observation is consistent with the recent international consensus on the definition of POP.<sup>8</sup> These criteria were not available when this study was planned. Subanalysis of the occurrence of musculo-fascial defects according to individual PFD symptoms is not part of the present work. A better correlation between POP signs and symptoms would probably be achieved using the evaluation criteria at the level of the hymen or beyond. We found that LAM defects in symptomatic women after first VD involved not only the PMC but also the ICM. We did not perform an isolated PRM evaluation within

P1. The PRM is a LAM subdivision that can be distinguished from the PMC. It originates also from the inner surface of the pubic bone lateral to the PMC and appears as a sling dorsal to the rectum. The PRM LAM subdivision has fiber directions that are oblique to the axial MRI scan plane, therefore the entire PRM loop is not visible in any one slice. The ventral attachment of the PRM can be assessed simultaneously with the evaluation of the ventral PMC attachment to the pubic bone. Based on our observations, it is mostly seen in the three distal MRI slices below the APL. The dorsal PRM bulk around the anal canal is mostly seen in the three proximal slices above the APL.

The proportion of cases with major LAM defects was significantly higher than observed in the parity-matched controls. The fact that 97.1% of bilateral major PMC defects were associated with bilateral major ICM defects demonstrates that the whole LAM, not only the PMC subdivision, may be involved in the muscular birth-related injuries. In the case of an unaffected PMC structure in symptomatic women, there is still a 66.7% probability of an ICM defect.

TABLE 1 Demographics, obstetric details, PFD symptoms, POP-Q staging of a POP-Q points comparison of study subjects

Selected demographic, obstetrics and urogynecologic data				
Parameter	Symptomatic (n = 149)	Asymptomatic (n = 60)	p	Obsv. power
Demographic and obstetric details				
Maternal age at delivery (yr)	31.8 ± 4.1	30.4 ± 3.8	0.000 <sup>c</sup>	0.586 <sup>f</sup>
Maternal age at examination (yr)	34.7 ± 5.1	30.1 ± 3.6	0.003 <sup>c</sup>	1.000 <sup>f</sup>
BMI (kg/m <sup>2</sup> )	23.6 ± 3.6	26.6 ± 3.5	0.000 <sup>c</sup>	1.000 <sup>f</sup>
Neonatal birthweight (g)	3521 ± 434.6	3533 ± 505.3	0.865 <sup>c</sup>	0.053 <sup>f</sup>
Type of vaginal delivery				
Spontaneous	123/149 (82.6)	60/60 (100)	0.003 <sup>d</sup>	0.882 <sup>h</sup>
Instrumental—forceps <sup>b</sup>	21/149 (14.1)	0/60 (0)		
Instrumental—vacuum	5/149 (3.4)	0/60 (0)		
Pelvic floor dysfunction symptoms				
Vaginal prolapse symptoms	95/149 (63.8)	0/60 (0)		
Urinary incontinence symptoms	20/149 (13.4)	0/60 (0)		
Dyspareunia/vaginal laxity	25/149 (16.8)	0/60 (0)		
Anorectal dysfunction symptoms	9/149 (6.0)	0/60 (0)		
POP-Q staging				
POP stage 0	29/149 (19.5)	60/60 (100)	0.000 <sup>d</sup>	1.000 <sup>h</sup>
POP stage I	11/149 (7.4)	0/60 (0)		
POP stage II	89/149 (59.7)	0/60 (0)		
POP stage III	20/149 (13.4)	0/60 (0)		
POP stage IV	0/149 (0)	0/60 (0)		
POP-Q points				
Point Aa	-1.0 (-2.0 to 0.0)	-2.0 (-2.9 to 2.0)	0.000 <sup>e</sup>	1.000 <sup>g</sup>
Point Ba	-1.0 (-2.0 to 0.0)	-2.0 (-2.9 to 2.0)	0.000 <sup>e</sup>	1.000 <sup>g</sup>
Point C	-5.0 (-7.0 to 1.0)	-7.0 (-7.0 to -7.0)	0.000 <sup>e</sup>	1.000 <sup>g</sup>
Point Ap	-1.5 (-2.0 to 1.0)	-2.0 (-2.0 to -2.0)	0.000 <sup>e</sup>	0.999 <sup>g</sup>
Point Bp	-1.5 (-2.0 to 1.0)	-2.0 (-2.0 to -2.0)	0.000 <sup>e</sup>	0.999 <sup>g</sup>
gh	4.5 (4.0–5.0)	3.5 (3.5–4.0)	0.000 <sup>e</sup>	1.000 <sup>g</sup>
pb	3.8 (3.5–4.0)	3.7 (3.5–4.0)	0.010 <sup>e</sup>	0.336 <sup>g</sup>
TVL	9.9 (9.0–10.0)	8.8 (8.5–9.0)	0.000 <sup>e</sup>	0.947 <sup>g</sup>
POP localization <sup>a</sup>				
Anterior compartment only	19/120 (15.8)	0/60 (0)		
Central compartment only	4/120 (3.3)	0/60 (0)		
Posterior compartment only	12/120 (10.0)	0/60 (0)		
Anterior and central compartment	14/120 (11.7)	0/60 (0)		
Posterior and central compartment	1/120 (0.8)	0/60 (0)		
Anterior and posterior compartment	34/120 (28.3)	0/60 (0)		
All compartments	36/120 (30.0)	0/60 (0)		

Abbreviations: BMI, body mass index; POP, pelvic organ prolapse.

<sup>a</sup>Not included were 29 symptomatic women with PFD who did not develop POP.

<sup>b</sup>Simpson 5.4%, Breus 3.4%, Kjelland 5.4%.

<sup>c</sup>Student's *t*-test.

<sup>d</sup>Chi-square test.

<sup>e</sup>Mann-Whitney test.

<sup>f</sup>Observed power based on Student's *t*-test.

<sup>g</sup>Observed power based on Mann-Whitney test.

<sup>h</sup>Observed power is based on effect size equal to Cramer's *V*.

The justification for considering ICM separately from the PMC is because it is inserted differently. This observation expands the previous findings of DeLancey et al., who determined that LAM defects also involve the ICM, although less commonly (2%) in primiparous women.<sup>14</sup> Surprisingly, the present study revealed that, in the control group, 35% of women also developed a major ICM defect. This could potentially be due to anatomic reasons. The ICM portion forms a horizontal muscle sheath that arises from the arcus tendineus levator ani (ATLA).<sup>15</sup> This collagenous bundle connects the thin ICM portion to the pelvic sidewall and the ischial spine. This attachment pattern is in contrast to the medial margin of the PMC, where the thick muscle is directly attached to the bone via a strong fibrous enthesis.<sup>16</sup> Due to tensile stretch during vaginal delivery, the failure location would occur in the muscular portion and the thin ICM fibers could be more easily avulsed from their origin portion.

The LAM defect distribution analysis can facilitate the understanding of the clinical consequences of LAM trauma induced by vaginal birth. The LAM functional change depends on the region of muscle affected and is related to the line of action of its fibers. In the standing position, the PMC generates a strong force, maintaining urogenital hiatus closure and pelvic organ lifting against the action of gravity. When the muscle complex is no longer able to maintain

hiatal closure, the pressure difference between the abdominal high-pressure zone and the lower atmospheric pressure zone deforms the vaginal wall.<sup>17</sup> These observations may be supported by the results of the current study, where the abnormal PMC morphology was associated with an OR for POP of 22.2. The PMC has a substantial lifting component that contributes to perineal elevation in healthy women.<sup>18</sup> The proximally located ICM muscle fibers have a similar direction to that of the PMC, so they also contribute to some elevation.<sup>18</sup> We found that women with an isolated major ICM defect were less likely to have POP (OR 4.9) than were women with a major PMC defect alone. This might indicate that ICM contributes more to the lifting action. According to our data, in the case of bilateral major PMC trauma, the presence of the same type of injury at the level of ICM can also be expected. Therefore, from a clinical point of view it is useful to have information about ICM status.

AD demonstrates a CT disruption and MRI images of women with AD show significant lateral or posterior spill of the vagina from its normal position.<sup>4</sup> This phenomenon was found in 85.9% of symptomatic women. In controls, the incidence of AD was very low and none of the women had an AD at P1 and P2 together. It was found that women with POP had an OR of 29.1 and 16.9 of having an AD at P1 and P2, respectively, compared with proven normal pelvic organ support. Anterior vaginal wall prolapse is the most common form of POP. In the symptomatic cohort, the anterior-predominant prolapse was identified in 85.8% of women with abnormal POP-Q parameters. Causal CT detachment factors contributing to cystocele formation include paravaginal defect and damaged apical support.<sup>19</sup> In 92.2% of cases with anterior-predominant prolapse, AD was visible. This observation is consistent with the work of Huebner et al.<sup>4</sup> who found that women with anterior prolapse were more likely to have AD. The present data support the concept of paravaginal defect where the lateral vaginal wall is displaced from its normal position in women with anterior wall prolapse and AD is the surrogate marker for this phenomenon.<sup>20</sup>

Chen et al. reported how apical support together with LAM affect the size of anterior vaginal wall prolapse.<sup>21</sup> In the present study, it was found that 78.7% of women with abnormal point C showed abnormal USL appearance and that women with POP had an OR of 10.1 of having abnormal apical support. If compartments other than middle compartment were involved in the POP, abnormal USL morphology was detected in 24.4% of cases. When all three compartments were included in the POP, 91.7% of USL were affected. Five women in the controls with abnormal USL origin-insertion points did not develop apical POP because of the low incidence of LAM defect in this group. With normal LAM function, but impaired apical support, no displacement occurs, since the vaginal wall is not exposed to a pressure differential.

We have chosen the term FA injury to describe cases where AD is present together with the LAM defect. Based on MRI, anatomic and histologic studies, Kim et al. revealed two patterns of LAM injuries, Type I and Type II.<sup>22</sup> Type II injury involves detachment of the LAM from the pubic bone or obturator internus muscle, with a loss of the normal architecture of the pelvic sidewall.

**TABLE 2** Intraclass correlation coefficients for LAM and CT parameters at P1, P2 and P3 (test-retest series, 45 symptomatic and 31 asymptomatic MRI examinations). The values ranked between 0.59 and 0.96, with best agreement for the LAM and CT defects at P1 and P2. The lowest agreement concerned the evaluation of the left USL origin/insertion points (Table 2)

Interobserver agreement for LAM and CT parameters at P1, P2 and P3			
Plane	Parameter	ICC	95% CI
P1	LAM score (right)	0.96	0.94–0.97
	LAM score (left)	0.92	0.88–0.95
	AD presence (right)	0.62	0.46–0.74
	AD presence(left)	0.85	0.78–0.96
	FA presence (right)	0.75	0.63–0.83
	FA presence (left)	0.85	0.77–0.90
P2	LAM score (right)	0.93	0.89–0.96
	LAM score (left)	0.94	0.92–0.97
	AD presence (right)	0.87	0.79–0.91
	AD presence(left)	0.80	0.71–0.87
	FA presence (right)	0.87	0.79–0.91
	FA presence (left)	0.91	0.86–0.94
P3	USL origin/insertion points (right)	0.70	0.57–0.79
	USL origin/insertion points (left)	0.59	0.41–0.71

Abbreviations: AD, architectural distortion; CT, connective tissue; FA, full avulsion; ICC, intraclass correlation coefficient; LAM, levator ani muscle; P1, plane 1; P2, plane 2; P3, plane 3; USL, uterosacral ligaments.

TABLE 3 LAM trauma status, AD incidence and distribution and USL origin/insertion points visualization

Presence of LAM and CT defects according to LAM and CT tissue trauma assessment					
Parameter		Symptomatic (n = 149)	Asymptomatic (n = 60)	p	Obs. power
LAM trauma assessment (MRI grade)					
P1	No LAM defect (grade 0)	30/149 (20.1)	44/60 (73.3)	0.000 <sup>a,0</sup>	1.000 <sup>b</sup>
	Minor LAM defect (grade 1-3)	19/149 (12.8)	12/60 (20.0)		
	Major LAM defect	100/149 (67.1)	4/60 (6.7)		
	Bilateral (grade 4-6)	70/100 (70.0)	2/4 (50.0)		
	Unilateral (grade 3)	30/100 (30.0)	2/4 (50.0)		
	Right-sided	21/30 (70.0)	2/2 (100)		
	Left-sided	9/30 (30.0)	0/2 (0)		
P2	No LAM defect (grade 0)	10/149 (6.7)	7/60 (11.7)	0.000 <sup>a,1</sup>	1.000 <sup>b</sup>
	Minor LAM defect (grade 1-3)	8/149 (5.4)	32/60 (53.3)		
	Major LAM defect	131/149 (87.9)	21/60 (35.0)		
	Bilateral (grade 4-6)	105/131 (80.2)	19/21 (90.5)		
	Unilateral (grade 3)	26/131 (19.8)	2/21 (9.5)		
	Right-sided	19/26 (73.0)	2/2 (100)		
	Left-sided	7/26 (27.0)	0/2 (0)		
CT trauma assessment					
P1	AD absence	59/149 (39.6)	58/60 (96.7)	0.000 <sup>a,0</sup>	1.000 <sup>b</sup>
	AD presence	90/149 (60.4)	2/60 (3.3)		
	Bilateral AD	61/90 (67.8)	0/60 (0)		
	Unilateral AD	29/90 (32.2)	2/2 (100)		
	Right-sided	20/29 (68.9)	2/2 (100)		
	Left-sided	9/29 (31.1)	0/2 (0)		
P2	AD absence	25/149 (16.8)	55/60 (91.7)	0.000 <sup>a,0</sup>	1.000 <sup>b</sup>
	AD presence	124/149 (83.2)	5/60 (8.3)		
	Bilateral AD	91/124 (73.4)	0/60 (0)		
	Unilateral AD	33/124 (26.6)	5/60 (100)		
	Right-sided	23/33 (69.7)	3/5 (60.0)		
	Left-sided	10/33 (30.3)	2/5 (40.0)		
P3	Normal USL origin/insertion points	75/149 (50.3)	55/60 (91.4)	0.000 <sup>a,2</sup>	1.000 <sup>b</sup>
	Abnormal USL origin/insertion points	73/149 (49.0)	5/60 (8.3)		
	USL tissue is not detectable	1/149 (0.7)	0/60 (0)		
LAM and CT trauma assessment					
P1	FA absence	59/149 (39.6)	58/60 (96.7)	0.000 <sup>a,0</sup>	1.000 <sup>b</sup>
	FA injury	90/149 (60.4)	2/60 (3.3)		
	Bilateral	61/90 (67.8)	0/2 (0)		
	Unilateral	29/90 (32.2)	2/2 (100)		
	Right-sided	20/29 (69.0)	2/2 (100)		
	Left-sided	9/29 (31.0)	0/2 (0)		

(Continues)



TABLE 3 (Continued)

Presence of LAM and CT defects according to LAM and CT tissue trauma assessment					
Parameter		Symptomatic (n = 149)	Asymptomatic (n = 60)	p	Obs. power
P2	FA absence	25/149 (16.8)	55 (91.7)	0.000 <sup>a,0</sup>	1.000 <sup>b</sup>
	FA injury	124/149 (83.2)	5/60 (8.3)		
	Bilateral	91/124 (72.6)	0/5 (0)		
	Unilateral	33/124 (26.6)	5/5 (100)		
	Right-sided	23/33 (69.7)	3/5 (60.0)		
	Left-sided	10/33 (30.3)	2/5 (40.0)		

Abbreviations: AD, architectural distortion; CT, connective tissue; FA, full avulsion; LAM, levator ani muscle; MRI, magnetic resonance imaging; P1, plane 1; P2, plane 2; P3, plane 3; USL, uterosacral ligaments.

<sup>a</sup>Both Chi-square and Fisher-Freeman-Halton exact test.

<sup>b</sup>Observed power is based on effect size equal to Cramer's V.

TABLE 4 Logistic regression for POP development after first vaginal delivery in relation to morphologic abnormalities in muscle trauma or connective tissue trauma and its combination at P1 or P2 or P3.

Multivariable logistic regression analysis for POP development after first vaginal delivery					
Plane	Independent variable	OR	Odds ratio 95% interval	p	Obs. power
Muscle (support) tissue trauma <sup>a,b</sup>					
P1	Bilateral minor LAM trauma	3.5	1.30–9.39	0.013	1.000 <sup>d</sup>
	Unilateral/bilateral major LAM trauma	22.1	8.94–54.67	0.000	
P2	Bilateral minor LAM trauma	0.2	0.05–1.07	0.062	1.000 <sup>d</sup>
	Unilateral/bilateral major LAM trauma	4.9	1.51–15.71	0.008	
Connective (attachment) tissue trauma					
P1	Unilateral/bilateral AD	29.1	9.77–86.31	0.000	1.000 <sup>d</sup>
P2	Unilateral/bilateral AD	16.9	7.62–37.69	0.000	1.000 <sup>d</sup>
P3	Unilateral/bilateral USL	10.1	4.01–25.29	0.000	1.000 <sup>d</sup>
Muscle (support) and connective (attachment) tissue trauma <sup>b,c</sup>					
P1	Minor LAM trauma + normal CT	3.04	0.89–10.39	0.075	1.000 <sup>e</sup>
	FA (major LAM trauma + present AD)	14.41	4.03–51.63	0.000	
P2	Minor LAM trauma + normal CT	0.31	0.05–1.86	0.200	1.000 <sup>e</sup>
	FA (major LAM trauma + present AD)	3.99	0.92–1.19	0.063	
P3	Unilateral/bilateral USL trauma	7.3	2.15–24.79	0.001	1.000 <sup>e</sup>

Abbreviations: AD, architectural distortion; CT, connective tissue; FA, full avulsion; LAM, levator ani muscle; OR, odds ratio; P1, plane 1; P2, plane 2; P3, plane 3; POP, pelvic organ prolapse; USL, uterosacral ligaments.

<sup>a</sup>Each variable is used in separate model.

<sup>b</sup>The reference category is no trauma.

<sup>c</sup>The model contains all subsequent variables.

<sup>d</sup>Observed power based on OR.

<sup>e</sup>Observed power only for models with separate variables, since computation for complete model is difficult.

This is consistent with the characteristic abnormal appearance of the vagina in the same region where damage to the LAM is seen. Both elements responsible for normal pelvic organ anatomy are interconnected. If one of these structures is compromised by excessive stretch during vaginal birth, the input work cannot be transmitted to structures. Although these problems can occur independently, at least half of the women with a paravaginal defect have an abnormal LAM, and so both usually occur together.<sup>20</sup> In

the symptomatic group at P1 90% of FA injuries also showed the presence of AD. We found a strong correlation between AD and LAM defect grade. At P1, bilateral FA were associated with a bilateral major LAM defect in 98.4%. Only 1.6% presented FA with minor LAM defects. The principal FA MRI image at level P2 is the deconfiguration of the pelvic floor suspension and support structures, corresponding to the arcus tendineus fasciae pelvis and arcus tendineus levator ani (ATLA) simultaneous trauma. Bilateral

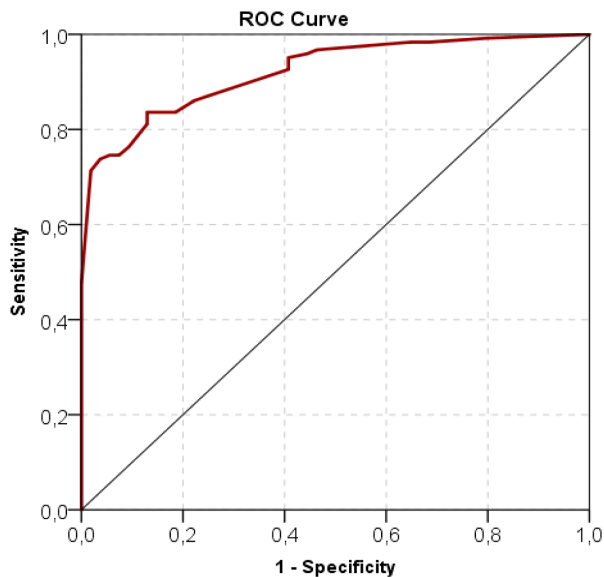


**FIGURE 3** Receiver operating characteristics curve of logistic regression model predicting presence of POP based on LAM (FA) and CT trauma evaluated at all three examinations of pelvic floor planes (P1, P2, P3) adjusted for maternal age. AUC = 0.921. ROC curve shows combination of the proportion of correctly diagnosed positive patients (Sensitivity) and the proportion of incorrectly diagnosed negative patients (1-Specificity). Each point of the curve was diagnosed using different threshold levels, which the output of the model has to exceed for the patient to be diagnosed as positive. AUC is a measure of model quality; range between 0 and 1 with 1 meaning a perfect ability of the model to distinguish event occurrence and non-occurrence of symptomatic and asymptomatic patients. AUC, area under the curve; CT, connective tissue; FA, full avulsion; LAM, levator ani muscle; P1, plane 1; P2, plane 2; P3, plane 3; POP, pelvic organ prolapse; ROC, receiver operating characteristics curve

FA at P2 was associated with bilateral major LAM defect in all women (100%). We found 10.8% cases with some degree of LAM defect without AD. These data demonstrate that defects of FA injuries at the level of PMC and ICM occur together with CT damage. The FA image at level P1 could be related to both PMC and PRM ventral attachment defect.

The LAM defect grading is an important POP risk factor published by Berger et al. in 2014.<sup>23</sup> He suggests that women with scores 3–5 are at moderate risk, and those with the score of 6 have the highest risk. In Type I injury, the LAM may be damaged locally, which in turn leads to muscle atrophy. Some substance of the muscle is lost but the levator arch remains intact.<sup>22</sup> Another possible explanation for this type of injury is denervation.<sup>14</sup> In the symptomatic group at P1, 39.6% of women without AD showed the presence of LAM defect. In this subgroup, significant lateral or posterior spill of the vagina from its normal position was not found. FA is also associated with increased risk of POP development.<sup>1</sup> The present study found that women with POP have an OR of 14.41 and 3.99 of having FA at P1 and P2, respectively, compared with proven normal pelvic organ support. Women with abnormal POP-Q parameters for anterior-predominant prolapse

were more likely to develop FA at P1 and P2 (71.1%). When FA was not found, anterior-predominant prolapse occurred in 27.9%. This demonstrates that the anterior vaginal wall support system involves a complex interaction between muscular and CT protecting the vagina, urethra and rectum from descent.<sup>20</sup>

The strengths of the study lie primarily in the large cohort of women with PFD after first spontaneous VD. A homogeneous cohort consisting of only ethnic caucasian women is a good representation of the local population. Further strengths are the use of standardized 3 Tesla MRI imaging protocol as well as intraobserver blinding to subject POP-Q and PFD symptom status.

The methodology of the present study has several limitations. This was not a population-based study and the control group was preselected, so the findings cannot be used to estimate the prevalence of muscular-fascial defects in the general population. Secondly, the investigators were not blinded to the LAM status at the time of AD evaluation, as it is not technically possible to deflect the LAM structure. This might represent a bias. Thirdly, only the axial images were used for USL assessment, since coronal images show better transition points for apical support visualization. Finally, MRI was not performed on all women at the same time interval postpartum.

The present study provides a detailed morphologic description of pelvic floor birth-related injuries. During the last 10–15 years, general MRI descriptions of the LAM and CT appearance of each individual level were published;<sup>4,7,11–14</sup> however, the details were not always appropriate, which has now been rectified in the current study. The findings of the present study provide accurate knowledge of anatomic failure sites, which is necessary for adequate therapeutic intervention in women with PFD.

## 5 | CONCLUSION

Birth-induced changes were also observed in asymptomatic controls but were less significantly pronounced. In women with PFD and proven bilateral major PMC trauma, the presence of the same type of injury at the level of ICM can be also expected. FA was associated with abnormal appearance of the vagina on MRI axial scans. Not only the muscle but also the CT are responsible for pelvic organ attachment becoming defective. The presence of AD indicates that CT and some degree of muscle defect has always been present. LAM defects may also occur in the absence of CT defects. In this type of muscular injury, some bulk of the muscle is lost; however, the levator arch remains intact. Due to the limitations of this study, generalization of the results should be made with care.

## CONFLICT OF INTEREST

None.

## AUTHOR CONTRIBUTIONS

M.K.: data collection/analysis, manuscript writing. L.H.: data collection. M.N.: data collection/analysis. P.H.: data collection. J.F.: editing. L.K.: data collection/analysis, manuscript writing, editing.

## FUNDING INFORMATION

This study was supported by the Charles University research project PROGRES.

## ORCID

Ladislav Krofta  <https://orcid.org/0000-0002-4372-3394>

## REFERENCES

1. Abdool Z, Shek K, Dietz H. The effect of levator avulsion on hiatal dimensions and function. *Am J Obstet Gynecol*. 2009;201:89.e1-89.e5.
2. Dietz HP. Forceps: towards obsolence or revival? *Acta Obstet Gynecol Scand*. 2015;94:347-351.
3. Swenson CW, Masteling M, DeLancey J, Nandikanti L, Schmidt P, Chen L. Aging effects on pelvic floor support: a pilot study comparing young vs older nulliparous women. *Int Urogynecol J*. 2019;31:535-543.
4. Huebner M, Margulies RU, DeLancey JOL. Pelvic architectural distortion is associated with pelvic organ prolapse. *Int Urogynecol J*. 2008;19:863-867.
5. Morgan MD, Umek W, Stein T, Hsu Y, Guire K, JOL DL. Interrater reliability of assessing levator ani muscle defects with magnetic resonance images. *Int Urogynecol J*. 2007;18:773-778.
6. Chen L, Lisse S, Larson K, Berger M, Ashton-Miller JA, JOL DL. Structural failure sites in anterior vaginal wall prolapse. *Obstet Gynecol*. 2016;128:853-862.
7. Larson KA, Luo J, Yousuf A, Ashton-Miller JA, JOL DL. Measurement of the 3D geometry of the fascial arches in women with a unilateral levator defect and "architectural distortion". *Int Urogynecol J*. 2012;23:57-63.
8. Haylen BT, de Ridder D, Freeman RM, et al. An international Urogynecological association (IUGA)/ international continence society (ICS) joint report on the terminology for female pelvic floor dysfunction. *Int Urogynecol J*. 2010;21:5-26.
9. Chou Q, JOL DL. A structured system to evaluate urethral support anatomy in magnetic resonance images. *Am J Obstet Gynecol*. 2001;185:44-50.
10. Strohbehn K, Ellis JH, Strohbehn JA, JOL DL. Magnetic resonance imaging of the levator ani with anatomic correlation. *Obstet Gynecol*. 1996;87:277-285.
11. DeLancey JOL, Morgan DM, Fenner DE, et al. Comparison of levator ani muscle defects and function in women with and without pelvic organ prolapse. *Obstet Gynecol*. 2007;109:295-302.
12. Umek WH, Morgan DM, Ashton-Miller JA, JOL DL. Quantitative analysis of uterosacral ligament origin and insertion points by magnetic resonance imaging. *Obstet Gynecol*. 2004;103:447-451.
13. Huebner M, DeLancey JOL. Levels of pelvic floor support: what do they look like on magnetic resonance imaging? *Int Urogynecol J*. 2019;30:1593-1595.
14. DeLancey JOL, Kearney R, Chou Q, Speights S, Binno S. The appearance of levator ani muscle abnormalities in magnetic resonance images after vaginal delivery. *Obstet Gynecol*. 2003;101:46-53.
15. Ashton-Miller JA, DeLancey JO. Functional anatomy of the female pelvic floor. *Ann N Y Acad Sci*. 2007;1101:266-296.
16. Kim J, Ramanah R, DeLancey JO, Ashton-Miller JA. On the anatomy and histology of the pubocervical muscle entheses in women. *NeuroUrol Urodyn*. 2011;30:1366-1370.
17. Chen L, Ashton-Miller JA, Hsu Y, JOL DL. Interaction between apical supports and levator ani in anterior vaginal support: theoretical analysis. *Obstet Gynecol*. 2006;108:324-332.
18. Betschart C, Kim J, Miller JM, Ashton-Miller JA, JOL DL. Comparison of muscle fibre directions between different levator ani muscle subdivisions: in vivo MRI measurements in women. *Int Urogynecol J*. 2014;25:1263-1268.
19. Larson KA, Luo J, Guire KE, Chen L, Ashton-Miller JA, JOL DL. 3D analysis of cystoceles using magnetic resonance imaging assessing midline, paravaginal, and anal apical defects. *Int Urogynecol J*. 2012;23:285-293.
20. Arenholt TS, Pedersen BG, Glavind K, Glavind-Kristensen M, JOL DL. Paravaginal defect: anatomy, clinical findings, and imaging. *Int Urogynecol J*. 2017;28:661-673.
21. Chen L, Ashton-Miller JA, Hsu Y, JOL DL. Interaction between apical supports and levator ani in anterior vaginal support: theoretical analysis. *Obstet Gynecol*. 2006;108:324-332.
22. Kim J, Betschart C, Ramanah R, Ashton-Miller JA, JOL DL. Anatomy of the pubocervical muscle origin: macroscopic and microscopic findings within the injury zone. *NeuroUrol Urodyn*. 2015;34:774-780.
23. Berger MB, Morgan DM, JOL DL. Levator ani defect scores and pelvic organ prolapse: is there a threshold effect? *Int Urogynecol J*. 2014;25:1375-1379.

**How to cite this article:** Krcmar M, Horcicka L, Nemeč M, Hanulíková P, Feyereisl J, Krofta L. Multilevel musculo-fascial defect magnetic resonance study of female pelvic floor: retrospective case control study in women with pelvic floor dysfunction after the first vaginal delivery. *Acta Obstet Gynecol Scand*. 2022;101:628-638. doi: [10.1111/aogs.14344](https://doi.org/10.1111/aogs.14344)